Journal of Theoretical Biology ■ (■■■■) ■■■–■■■

Contents lists available at SciVerse ScienceDirect

Journal of Theoretical Biology

journal homepage: www.elsevier.com/locate/yjtbi

In vivo, *in vitro*, and *in silico* studies suggest a conserved immune module that regulates malaria parasite transmission from mammals to mosquitoes

Ian Price [a], Bard Ermentrout [a,c], Ruben Zamora [b,c], Bo Wang [d], Nabil Azhar [b,c,e], Qi Mi [c,f], Gregory Constantine [a,c], James R. Faeder [c,e], Shirley Luckhart [d], Yoram Vodovotz [b,c,*]

[a] Department of Mathematics, University of Pittsburgh, Pittsburgh, PA 15260, United States
[b] Department of Surgery, University of Pittsburgh, Pittsburgh, PA 15213, United States
[c] Center for Inflammation and Regenerative Modeling, McGowan Institute for Regenerative Medicine, University of Pittsburgh, Pittsburgh, PA 15219, United States
[d] Department of Medical Microbiology and Immunology, University of California-Davis, Davis, CA 95616, United States
[e] Department of Computational and Systems Biology, University of Pittsburgh, Pittsburgh, PA 15260, United States
[f] Department of Sports Medicine and Nutrition, University of Pittsburgh, Pittsburgh, PA 15260, United States

HIGHLIGHTS

- Malaria is caused by *Plasmodium falciparum* and transmitted by *Anopheles* mosquitoes.
- Mammalian transforming growth factor-β1 (TGF-β1) is ingested during bloodfeeding.
- Ingested TGF-β1 signals in the mosquito via MEK/ERK.
- Models and experiments were carried out on this "immunological crosstalk".
- These studies suggested multiphasic behavior of key anti-parasite effectors.

ARTICLE INFO

Article history:
Received 22 February 2013
Received in revised form
24 May 2013
Accepted 31 May 2013

Keywords:
Malaria
Mathematical model
Transforming growth Factor-β1
Nitric oxide
Mitogen-activated protein kinase
Computational biology

ABSTRACT

Human malaria can be caused by the parasite *Plasmodium falciparum* that is transmitted by female *Anopheles* mosquitoes. "Immunological crosstalk" between the mammalian and anopheline hosts for *Plasmodium* functions to control parasite numbers. Key to this process is the mammalian cytokine transforming growth factor-β1 (TGF-β1). In mammals, TGF-β1 regulates inducible nitric oxide (NO) synthase (*iNOS*) both positively and negatively. In some settings, high levels of NO activate latent TGF-β1, which in turn suppresses *iNOS* expression. In the mosquito, ingested TGF-β1 induces *A. stephensi* NOS (*AsNOS*), which limits parasite development and which in turn is suppressed by activation of the mosquito homolog of the mitogen-activated protein kinases MEK and ERK. Computational models linking TGF-β1, *AsNOS*, and MEK/ERK were developed to provide insights into this complex biology. An initial Boolean model suggested that, as occurs in mammalian cells, MEK/ERK and *AsNOS* would oscillate upon ingestion of TGF-β1. In support of this hypothesis, statistical models of multiphasic behavior were a best fit for data derived from time courses of *Anopheles* ERK activation *in vitro* and of *AsNOS* expression *in vivo* following treatment with TGF-β1. An ordinary differential equation (ODE) model further supported the hypothesis of TGF-β1-induced multiphasic behavior of MEK/ERK and *AsNOS*. To achieve this multiphasic behavior, the ODE model was predicated on the presence of constant levels of TGF-β1 in the mosquito midgut. Ingested TGF-β1, however, did not exhibit this behavior. Accordingly, we

Abbreviations: As60A, *Anopheles stephensi* 60A; ERK, extracellular signal-regulated kinase; JNK, Jun *N*-terminal kinase; NO, nitric oxide; NOS, nitric oxide synthase; AsNOS, *Anopheles stephensi* NOS; iNOS, mammalian inducible NOS; MAPK, mitogen-activated protein kinase; MEK, ERK kinase kinase; p38 MAPK, MAPK of 38 kilo Dalton molecular weight; ODE, ordinary differential equation; PBS, phosphate-buffered saline; RNS, reactive nitric oxide species; TGF-β1, transforming growth factor-β1.

* Corresponding author at: University of Pittsburgh, Department of Surgery, W944 Starzl Biomedical Science Tower, 200 Lothrop St., Pittsburgh, PA 15213, United States. Tel.: +1 412 647 5609; fax: +1 412 383 5946.
E-mail address: vodovotzy@upmc.edu (Y. Vodovotz).

0022-5193/$ - see front matter © 2013 Published by Elsevier Ltd.
http://dx.doi.org/10.1016/j.jtbi.2013.05.028

hypothesized and experimentally verified that ingested TGF-β1 induces the expression of the endogenous mosquito TGF-β superfamily ligand *As60A*. Computational simulation of these complex, cross-species interactions suggested that TGF-β1 and NO-mediated induction of *As60A* expression together may act to maintain multiphasic *AsNOS* expression via MEK/ERK-dependent signaling.

We hypothesize that multiphasic behavior as represented in this model allows the mosquito to balance the conflicting demands of parasite killing and metabolic homeostasis in the face of damaging inflammation.

1. Introduction

1.1. Malaria and the role of "immunological crosstalk" between mammalian host and mosquito vector

Half of the global population is at risk for malaria, which results in nearly 1 million deaths annually, 86% of which are in children (WHO. World Malaria Report, 2011). *Plasmodium falciparum*, the most important human malaria parasite, is transmitted by female *Anopheles* mosquitoes. Parasite development in the mosquito begins with the ingestion of blood containing sexual-stage gametocytes. Mobile ookinetes penetrate the midgut epithelium 24–36 h later and transform into midgut-bound oocysts within the open circulatory system of the mosquito. Oocysts grow and develop for 10–12 days and then release thousands of sporozoites, which invade the salivary glands and are released during later blood feeding.

The mosquito is not a neutral vector of transmission, but rather ingests blood components including immune-modulating factors from the infected mammalian host (Akman-Anderson et al., 2007; Pakpour et al., 2013) (Fig. 1). Ingestion of these blood components impacts the ability of the mosquito to kill *Plasmodium* parasites by altering the immune/inflammatory environment, and thus impacts this individual outcome as well as overall transmission of malaria infection. The impact of this "immunological crosstalk" on parasite transmission, therefore, requires an understanding of the complex blood-feeding interface among the mammalian host, the mosquito and the malaria parasites that utilize both of these hosts for biological development.

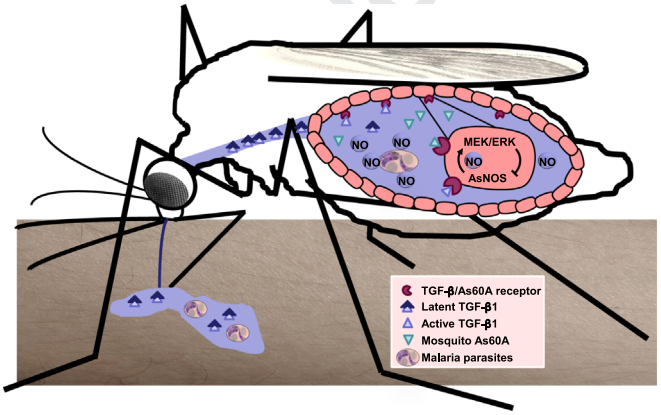

Fig. 1. Host-vector molecular crosstalk in malaria. *Anopheles* mosquitoes ingest blood components including cytokines such as TGF-β1 upon bloodfeeding. TGF-β1, which exists predominantly in its latent form in mammalian host blood, becomes activated in the mosquito midgut in a process that is driven by the mosquito NO-producing enzyme, AsNOS. Locally high AsNOS-derived NO levels in the midgut lumen kill *Plasmodium* parasites. At a signaling level, TGF-β1-induced oscillations in AsNOS-derived NO activate the signaling kinases MEK and ERK. In particular, AsNOS-derived NO activates the expression of *As60A*, which maintains a TGF-β1-like influence in the midgut after degradation of active TGF-β1. Activation of MEK and ERK signaling, among many other effects, drives multiphasic regulation of *AsNOS* expression and AsNOS activity, perhaps in an effort to balance the conflicting demands of parasite killing and homeostasis in the face of damaging inflammation.

1.2. The mammalian cytokine transforming growth factor-β1 is a key molecule in "immunological crosstalk" that regulates malaria parasite infection via nitric oxide production

One of these "crosstalking" factors is the cytokine transforming growth factor-β1 (TGF-β1). In mammals, TGF-β1 is produced as an inactive precursor that is activated following dissociation of inhibitory proteins. This process can be promoted by reaction products of the free radical nitric oxide (NO), which are in turn generated by catalytic activity of NO synthase (NOS) isoforms, including an inducible isoform (iNOS) commonly associated with host defense responses. In some immune cells, TGF-β1 reduces iNOS activity, expression, mRNA stability, translation, and protein stability; in other cell types TGF-β1 can upregulate *iNOS* expression and iNOS enzyme activity (Gilbert and Herschmann, 1993; Goureau et al., 1993; Blanco et al., 1995; Vodovotz, 1997; Vodovotz et al., 2004). This upregulation results in continued synthesis of NO (Blanco et al., 1995), which in turn has the potential to induce synthesis of additional TGF-β1 (Kim et al., 1989a, 1989b, 1989c), thereby yielding a cycle of positive feedback regulation.

TGF-β1 is a pleiotropic cytokine (Wahl, 2007) that plays a pivotal role during malaria parasite infection and, therefore, may maintain an "immunological balance" in this context (Omer et al., 2000, 2003; Dodoo et al., 2002; Dunachie et al., 2010). The regulation of iNOS by TGF-β1 is central to this balance and to the effects of TGF-β1 on parasite infection (Vodovotz et al., 2004). During *Plasmodium* infection in humans and mice, NO can inactivate sporozoites and circulating gametocytes (Naotunne et al., 1993; Mellouk et al., 1994), and various studies have reported both beneficial and detrimental effects of NO on the pathology of infection (Anstey et al., 1996; Clark et al., 2004).

The control of malaria parasite infection by inducible NO synthesis in a mosquito was first described in *Anopheles stephensi* (Luckhart et al., 1998), a major malaria vector in India, southeast Asia and parts of the Middle East. The induction of *A. stephensi NOS* (*AsNOS*) expression in the midgut is biphasic. Specifically, greater than two-fold inductions of *AsNOS* were observed at 1–6 h and at 36–48 h after malaria parasite infection (Luckhart et al., 2003) and after bloodfeeding with parasite glycosylphosphatidylinositols, major parasite signaling inducers that are highly active in mammals as well (Lim et al., 2005). These inductions result in the catalysis of inflammatory levels of toxic nitrogen oxides in the mosquito midgut (Luckhart et al., 1998; Peterson et al., 2007).

Given the extreme conservation of TGF-β signaling in metazoans (Roberts and Sporn, 1990, 1996; Attisano and Lee-Hoeflich, 2001), we focused on TGF-β1 as a possible regulatory mediator of *AsNOS* expression and NO synthesis. Upon bloodfeeding, *A. stephensi* ingests circulating latent TGF-β1 from the mammalian host (Fig. 1). Ingested TGF-β1 is activated rapidly in the midgut post-bloodfeeding (Luckhart et al., 2003). *In vitro*, latent TGF-β1 is not activated by midgut lysates alone, but is activated after incubation with midgut lysates in the presence of an NO donor to simulate NO synthesis following bloodfeeding (Luckhart et al., 2003) (Fig. 1). We found that low levels of human TGF-β1 (2 pg/ml) provided in blood inhibited *P. falciparum* growth in *A. stephensi*, while a higher dose (2000 pg/ml) did not affect parasite growth,

Please cite this article as: Price, I., et al., *In vivo*, *in vitro*, and *in silico* studies suggest a conserved immune module that regulates malaria parasite transmission from mammals to mosquitoes. J. Theor. Biol. (2013), http://dx.doi.org/10.1016/j.jtbi.2013.05.028

suggesting an anti-inflammatory or dampening effect on mosquito defenses against parasite infection (Luckhart et al., 2003). We therefore hypothesized that TGF-β1 could exert dichotomous, dose-dependent effects on *AsNOS* expression *in vivo* and on AsNOS catalytic activity during malaria parasite infection in the mosquito. Our data confirmed this hypothesis, indicating that while both low and high doses of human TGF-β1 could induce *AsNOS* expression, only the lower doses resulted in higher, sustained induction of anti-parasitic *AsNOS* (Luckhart et al., 2008). We also confirmed that catalytic activity of AsNOS regulates *AsNOS* expression and TGF-β1-associated killing of developing parasites (Luckhart et al., 2008).

1.3. TGF-β1/nitric oxide signal via the mitogen-activated protein kinase pathway in anopheles mosquitoes

Similar to the case in the mammalian host, downstream signaling responses must be moderated to prevent excessive, NO-mediated damage to the mosquito host. One key intracellular signaling mechanism involves one or more of the three mitogen-activated protein kinases (MAPK), including the Jun *N*-terminal kinase (JNK), extracellular signal-regulated kinase (ERK), and p38 MAPK pathways, all of which regulate cellular processes through phosphorylation of target substrates (Kyriakis and Avruch, 2012). Each of these enzymes is itself regulated via phosphorylation by upstream kinases (so-called 'kinase kinases'); in the case of ERK, this upstream enzyme is known as MEK (Kolch, 2000). We demonstrated that TGF-β1-dependent MEK/ERK signaling negatively regulates *AsNOS* expression (Surachetpong et al., 2009). That is, at the highest treatment dose of TGF-β1, inhibition of MEK/ERK phosphorylation increased TGF-β1-induced *AsNOS* expression, suggesting that increasing levels of MEK/ERK activation negatively feedback on induced *AsNOS* expression (Fig. 1). Interestingly, residual NO may induce tyrosine nitration of ERK, which has been demonstrated to activate ERK in mammalian cells (Pinzar et al., 2005), further enhancing negative feedback on *AsNOS* expression. Reactive NO species (RNS), formed through reactions between NO and reactive oxygen species (ROS), also modulate MAP kinase signaling (Levonen et al., 2001), regulation that is mirrored by ROS-dependent activation of MEK/ERK signaling in *A. stephensi* cells (Surachetpong et al., 2011). Inhibition of MEK/ERK activation enhanced TGF-β1-mediated control of *P. falciparum* development, demonstrating that MEK/ERK signaling moderates the biological effects of ingested TGF-β1 (Surachetpong et al., 2009) likely through feedback regulation by RNS (Fig. 1).

1.4. Deriving insights into malaria via computational modeling of immunological "crosstalk"

Taken together, the interactions within the TGF-β1-NOS-NO axis in the context of malaria parasite infection in *A. stephensi* include complexities of timing, dose-dependent effects, feedback regulation, multiple inducers of single targets, and multiple targets of single regulatory factors (Fig. 1). We hypothesized that computational simulation of this system would yield novel basic and translational insights into the biology, pathology, and ecology of malaria transmission. Accordingly, we obtained data on the dynamics of MEK/ERK *in vitro* and *AsNOS in vivo* in mosquitoes in response to exposure to mammalian TGF-β1 to create statistical, logical, and ordinary differential equation (ODE) mathematical models to account for the main observed components of the response to ingested TGF-β1. Taken together, our experimental and computational studies suggest the possibility of multiphasic expression of *AsNOS* based on induction via TGF-β1 and suppression via MEK/ERK signaling, and further suggest that this multiphasic expression requires, in some settings, the NO-dependent, TGF-β1-induced expression of the *A. stephensi* homolog of TGF-β1, As60A. Further experiments are needed to verify the presence of and mechanisms for the multiphasic behavior of this biological system, which may allow the mosquito to balance the conflicting demands of parasite killing and maintaining homeostasis in the face of damaging inflammation.

2. Materials and methods

2.1. Boolean model of inter-species "immunological crosstalk"

In modeling the mosquito-mammal "immunological crosstalk", the relevant biochemical interactions were depicted graphically as an influence diagram (Fig. 2A). This diagram suggested that these interactions comprise an activator-inhibitor system, with the activation mediated through the ingestion of exogenous TGF-β1. To gain an initial understanding of the qualitative behavior of this system, a Boolean model was constructed using BooleanNet, an open-source platform for Boolean model construction and simulation (Albert et al., 2008). The network was coded with the simplified topology depicted in Fig. 2B (model code is detailed in the *Supplementary materials*). The dynamical equations for the Boolean model are given by the functions

$$\mathrm{AsNOS}^* = \mathrm{TGF}{-}\beta 1 \text{ AND NOT MEK/ERK}$$
$$\mathrm{RNS}^* = \mathrm{AsNOS}$$
$$\mathrm{ERK}^* = \mathrm{RNS}$$

where each variable takes one of two values – ACTIVE or INACTIVE – and the symbol '*' indicates the value of a variable at the next time point. The state of the system at a given time can be represented by a four-element vector of ones and zeroes representing the value (ACTIVE or INACTIVE, respectively) of each of the four variables in the order (TGF-β1, AsNOS, RNS, ERK). The initial state of the model, taken to be when TGF-β1 is ACTIVE while the remaining components are inactive, is represented by the vector (1 0 0 0), which forms the stable limit cycle

$$(1\,0\,0\,0) {-}{>} (1\,1\,0\,0) {-}{>} (1\,1\,1\,0) {-}{>} (1\,1\,1\,1) {-}{>} (1\,0\,1\,1) {-}{>} (1\,0\,0\,1) {-}{>} (1\,0\,0\,0)$$

Because of the simplicity of the model, the update semantics (asynchronous or synchronous) yield the same dynamics.

2.2. Ordinary differential equation model of inter-species "immunological crosstalk"

Based on insights from the Boolean model and in order to gain insights into regimes of behavior and relevant parameters of this "immunological crosstalk" system, a second model was created using ordinary differential equations (ODE), based on the conceptual model depicted in Fig. 2C, a simplification of Fig. 2A. The system was modeled as an nonlinear activator-inhibitor system (Edelstein-Keshet, 2005; Murray, 2002). In this model, *AsNOS* (N) has a constant baseline production and degradation, as well as production induced by auto-induction of strength α, representing the signaling as up-regulated via the long-term contributions of the TGF-β1 pathway. This induction is also competitively inhibited by a MEK/ERK (X) signaling pathway. RNS is not included as an intermediary because the well-mixed property of ODE systems would make this proportional to MEK/ERK. The equation for MEK/ERK similarly has degradation and production based on a saturating function of *AsNOS* (Eq. (1)):

$$\frac{dN}{dt} = \mu_N(b_N - N) + \frac{\alpha N^p}{N^p + a_{NX}X^q + a_N^p} \quad \frac{dX}{dt} = -\mu_X X + \frac{b_{XN}N}{a_{XN} + N} \tag{1}$$

The variables and parameters are written to be unitless. Of the two variables, we could only obtain data for one variable, *AsNOS*

Please cite this article as: Price, I., et al., *In vivo*, *in vitro*, and *in silico* studies suggest a conserved immune module that regulates malaria parasite transmission from mammals to mosquitoes. J. Theor. Biol. (2013), http://dx.doi.org/10.1016/j.jtbi.2013.05.028

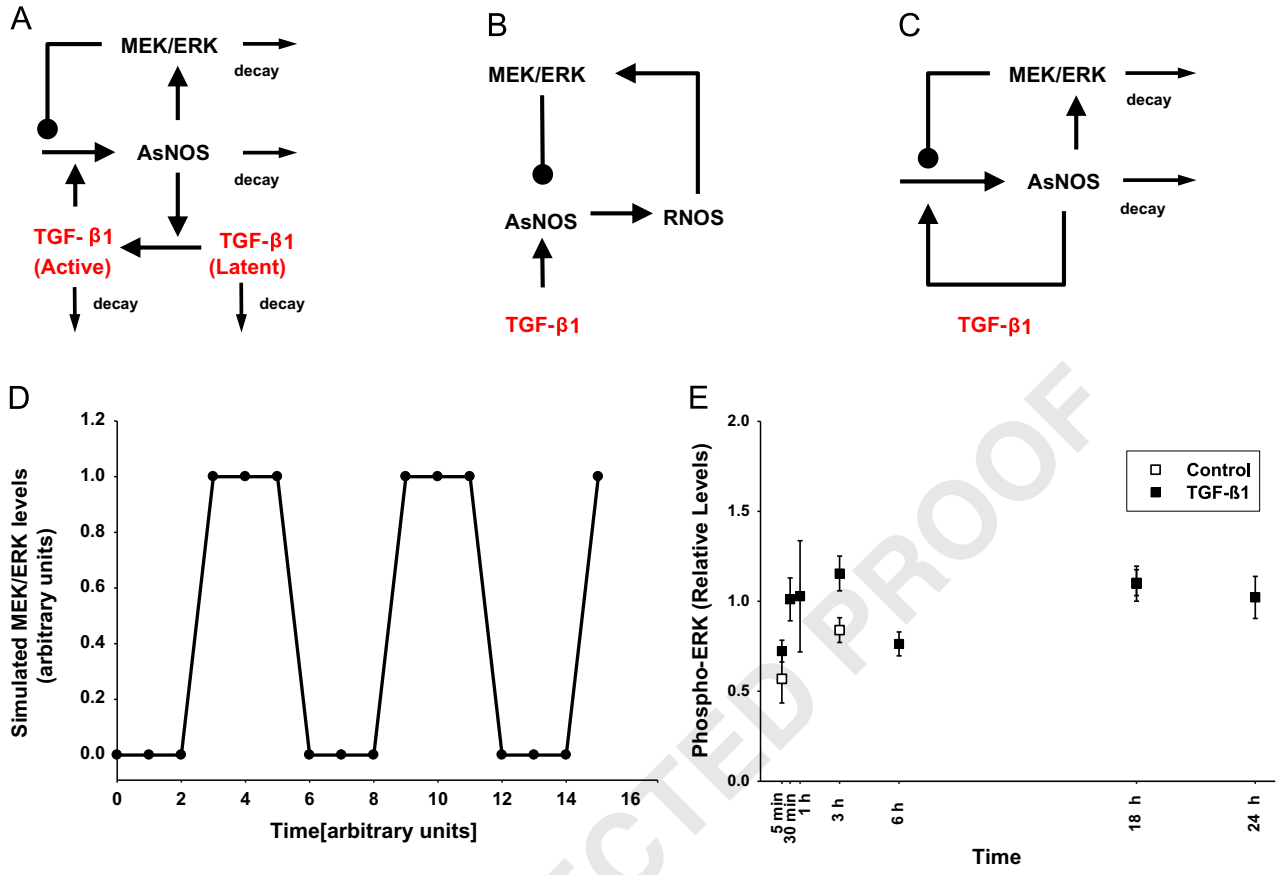

Fig. 2. Computational modeling of TGF-β1 – AsNOS – MEK/ERK interactions suggests, and *in vitro* studies support, multiphasic behavior of MEK/ERK signaling. *Panel A*: Schematic of hypothesized interactions among ingested mammalian TGF-β1 (red text indicates host-derived molecule), mosquito AsNOS, and mosquito MEK/ERK signaling (black text indicates mosquito-derived molecules and processes). *Panel B*: Schematic of interactions similar to *Panel A*, used to create a Boolean model of cross-species interactions as described in Section 2 and *Supplementary materials*. *Panel C*: Simplification of *Panel A*, used to create an ODE model as described in Section 2 and *Supplementary materials*. Panels A–C: standard arrows indicate induction/activation/potentiation, and circle-tipped lines indicate suppression/inhibition. *Panel D*: Output of the Boolean model depicted schematically in *Panel B* suggests oscillations of phosphorylated (active) ERK induced by ingested mammalian TGF-β1. *Panel E*: *A. gambiae* 4a3B cells were stimulated with 6000 pg/ml human TGF-β1 (black squares, $n=6$–9 experiments) or vehicle control and phospho-ERK levels were analyzed as described in Section 2. (For interpretation of the references to color in this figure legend, the reader is referred to the web version of this article.)

(N) due to the scarcity of the midgut samples; therefore, we could not obtain data for MEK/ERK (X) in the same experiments. The data for N are the products of a normalization transformation which does not produce units in the output. Since the data are unitless, the corresponding variable and its parameters are designed to be unitless. The variable X and related parameters are designed to be unitless so as to be consistent.

This model is highly simplified, and lacks an explicit addition of TGF-β1; rather, the long term contributions of TGF-β1 are added implicitly as the parameter α, and the transient contributions via the initial conditions. The equations of the model therefore simplify the dynamics to focus continuously on the long-term response. To account for the transient dynamics of TGF-β1 in the cross-talk, the model assumes a static increase in expression of *AsNOS* at the time of the first measurement, time zero, determined from the experimental data. Between the time of the bloodmeal and the time of the initial measurement (approximately 30 min due to experimental constraints explained above), the relative expression levels of *AsNOS* for the 2 pg/ml and 2000 pg/ml cohorts compared to PBS increase in excess of two-fold and five-fold, respectively. The model assumes that these large rises *AsNOS* expression in the 30 min post bloodmeal are the predominant effect of transient TGF-β1 signaling, and for simplicity no further transient contributions are considered.

One possible behavior of this activator-inhibitor model is a stable limit cycle with an unstable equilibrium point (*Supplementary materials*, Fig. S1). For the parameter α, representing TGF-β1 induction, the region of the x-axis corresponding to open circles on the y-axis represents the values which produce stable limit cycles, i.e. oscillatory behavior. Below and above this region, the system undergoes Andronov–Hopf bifurcations, so that the system is attracted to a fixed value and may show excitability but no sustained oscillation. In the time-frame for which data were collected, a multiphasic pattern in the data points was assumed, which could be modeled by a stable limit cycle—implying either a true oscillation, or else a decaying oscillation with the decay not seen in the measured time frame.

Initial parameter fits for the individual time courses were achieved in the XPP equation solving program (Ermentrout, 2002) using the built-in Levenberg–Marquardt algorithm (Bertsekas, 1995). The global properties of the system were explored using the AUTO (Doedel, 1981) functionality to explore bifurcations in the parameter space; for the original code and graphs of characteristic one and two-parameter bifurcations, see *Supplementary materials* (Figs. S1 and S2). The initial parameter fits were used as the basis for the boundaries of the parameter space from which to choose new parameter fits (Table 1). These parameters include nine parameters universal to all three experiments, individual values of α for each of the three, individual values of initial *AsNOS*, and individual values of initial MEK/ERK, for a total of 18 values varied.

The three time-courses of data were simultaneously fit to data, so that a single model describes all three outcomes. An objective function was written as the sum of the squares of the differences between data and trajectory output divided by the standard error

Please cite this article as: Price, I., et al., *In vivo*, *in vitro*, and *in silico* studies suggest a conserved immune module that regulates malaria parasite transmission from mammals to mosquitoes. J. Theor. Biol. (2013), http://dx.doi.org/10.1016/j.jtbi.2013.05.028

Table 1
Names and biological meanings of ordinary differential equation model parameters.

Parameter	Initial Set	Bounds	Description	Assoc. E-Val (Rank)
μ_n	1.7	[1.4, 2.0]	AsNOS degradation	0.225 (6)
b_n	0.5	[0.4, 0.6]	Baseline AsNOS production	0.898 (13)
p	1.9	[1.6, 2.3]	Upregulation exponent	0.0653 (4)
a_n	5.7	[4.7, 6.8]	AsNOS regulatory term	0.0397 (3)
a_{nx}	1.4	[1.1, 1.6]	AsNOS inhibition term	0.225 (5)
q	1.7	[1.4, 2.0]	Inhibition exponent	2.90 (18)
μ_x	0.7	[0.58, 0.82]	MEK/ERK degradation	1.97 (17)
b_x	28	[23, 33]	MEK/ERK max. production	1.90 (16)
a_x	10.1	[8.1, 12]	MEK/ERK regulatory term	0.296 (6)
α_{PBS}	39	[39, 48]	AsNOS induction via TGF (PBS)	0.0133 (1)
α_2	43	[41, 52]	AsNOS induction via TGF (2 pg/ml)	0.0133 (1)
α_{2000}	50	[45, 60]	AsNOS induction via TGF (2000 pg/ml)	0.0308 (2)
$N_{PBS}^{(0)}$	1.1	[0.8, 1.3]	Initial condition (AsNOS)	1.90 (16)
$N_2^{(0)}$	1.6	[1.0, 2.3]	Initial condition (AsNOS)	1.23 (14)
$N_{2000}^{(0)}$	4	[2.0, 6.0]	Initial condition (AsNOS)	0.455 (8)
$X_{PBS}^{(0)}$	7.6	[5.5, 9.0]	Initial condition (MEK/ERK)	1.33 (15)
$X_2^{(0)}$	7.5	[5.5, 9.0]	Initial condition (MEK/ERK)	1.07 (13)
$X_{2000}^{(0)}$	7.9	[5.5, 9.0]	Initial condition (MEK/ERK)	1.07 (13)

Note 1: The eigenvalues of the rank correlation are ordered lowest (1) to highest (18), with importance increasing.
Note 2: There is no one to one correspondence between parameters and eigenvalues. For a given parameter, the most important value is given.

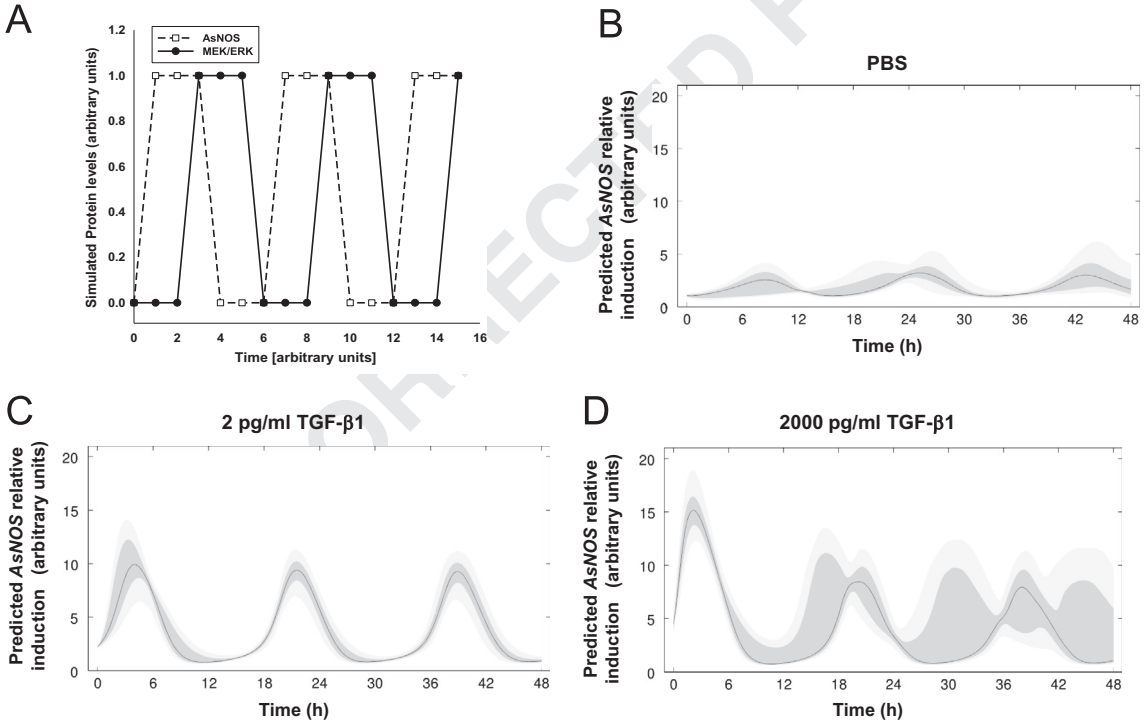

Fig. 3. Computational studies suggest multiphasic expression of TGF-β1-induced *AsNOS*. *Panel A*: The Boolean model depicted in Fig. 1B and D suggests that, like phospho-ERK, AsNOS also oscillates in response to ingestion of TGF-β1. *Panels B–D*: Ensembles of ODE model simulations of 0 pg/ml TGF-β1 (*Panel B*), 2 pg/ml TGF-β1 (*Panel C*), and 2000 pg/ml TGF-β1 (*Panel D*). Simulated *AsNOS* dynamics derived from an ensemble of simulations derived from a mechanistic ODE model are shown as quartiles of possible values taken at each time point, with the average as the black line, the inner 50% as dark grey, and the outer 90% as light grey.

of the data (Tarantola, 2005). This objective function was used inside a Metropolis–Hastings method with parallel tempering (Tarantola, 2005) to create an ensemble of parameter sets that fit the data with statistically similar probability. For the one-dimensional histograms of this ensemble, see *Supplementary material* (Fig. S3). Validation of the parameter sets was done through two filters: first that the values of α corresponding to the various doses were monotone increasing, and second that the value of α corresponding to PBS produce a stable limit cycle. The trajectories of this ensemble were graphed as quartiles of possible values taken at each time point (Fig. 3B–D) with the median as the black line, the inner 50% as dark grey, and the outer 90% as light grey. The ensemble of parameters was also used to compute the matrix of rank correlation between the values of the parameters, and Principal Component Analysis (Pearson, 1901) was performed to determine the individually important parameters of the system (Table 1).

2.3. Assessment of MEK/ERK signaling in anopheles cells in vitro

For these studies, we utilized immortalized 4a3B cells derived from minced larvae of *Anopheles gambiae*, a species that is closely related to *A. stephensi*. The 4a3B cells robustly exhibit TGF-β1-dependent signaling profiles that are identical to those of *A. stephensi*

Please cite this article as: Price, I., et al., *In vivo*, *in vitro*, and *in silico* studies suggest a conserved immune module that regulates malaria parasite transmission from mammals to mosquitoes. J. Theor. Biol. (2013), http://dx.doi.org/10.1016/j.jtbi.2013.05.028

cells (Surachetpong et al., 2011). 4a3B cells were maintained in Schneider's medium (Invitrogen, Carlsbad, CA) with 10% heat-inactivated fetal bovine serum at 28 °C. Briefly, 2×10^6 cells in 2 ml medium were plated in each well of 12 well tissue culture plates for 4 h. After experimental treatment with 6000 pg/ml TGF-β1 or with an equivalent volume of TGF-β1 diluent (4 mM HCl with 0.1% BSA) as a control for times ranging from 5 min to 24 h, culture media were removed and cells were washed with ice cold phosphate-buffered saline (PBS) and lysed in 100 μl cell lysis buffer (10 mM Tris–HCl pH 7.4, 1 mM EDTA, 100 mM NaCl, 1 mM NaF, 1 mM EGTA, 2 mM Na_3VO_4, 20 mM $Na_4P_2O_7$, 0.1% SDS, 1% Triton X-100, 0.5% sodium deoxycholate, 1 mM phenylmethylsulfonyl fluoride, 10% glycerol, 60 μg/ml aprotinin, 10 μg/ml leupeptin, 1 μg/ml pepstatin, and 1 μg/ml calyculin A). The plate was agitated for 30 min at 4 °C and samples were incubated on ice for 30 min. Cell lysates were centrifuged at 14,000 × *g* for 10 min at 4 °C to remove cellular debris and the resulting supernatants were mixed with sample buffer (125 mM Tris–HCl pH 6.8, 10% glycerol, 10% SDS, 0.006% bromophenol blue, 130 mM dithiothreitol) and heated to 95 °C for 4 min. Equivalent concentrations of proteins (as measured by BCA assay) were separated on 10% SDS-PAGE polyacrylamide gels and transferred to nitrocellulose membranes (BioRad). Protein loading was also visually assessed by Coomassie blue staining. Membranes were blocked in 5% nonfat dry milk (w/v) in 1 × Tris-buffered saline (TBS; pH 7.0) containing 0.1% Triton-100 (TBS-T) 1 h at room temperature. For phospho-ERK detection, membranes were incubated at 4 °C overnight with 1:10,000 mouse anti-phospho-ERK monoclonal antibody (Sigma Aldrich) or rabbit anti-GAPDH (Abcam) in 5% nonfat dry milk 1 × TBS-T. After washing three times for 5 min each, the membranes were incubated overnight at 4 °C with diluted secondary antibody (HRP-conjugated rabbit anti-mouse IgG or HRP-conjugated goat anti-rabbit (Fab')-2 fragment according to the host of the primary antibody). The membranes were then washed three times for 5 min each, followed by incubation with SuperSignal® West Pico chemiluminescent reagent for 2–5 min and exposure to blue autoradiography film. Phospho-ERK or GAPDH levels were measured and quantified by scanning the film on a GS-800 calibrated densitometer. Levels of phospho-ERK in treatment and control groups were normalized to loading control protein levels (GAPDH or total ERK). Three biological replicates were performed for each time point.

2.4. Studies in adult female Anopheles stephensi

The persistence of ingested mammalian TGF-β1 and the degree to which latent TGF-β1 is activated following ingestion by *A. stephensi* were determined using a rat blood model under an approved Institutional Animal Care and Use protocol. Specifically, blood from anesthetized albino white rats (SD strain) was collected with citrate-phosphate-dextrose-adenine (CPDA-1) anticoagulant and transferred to a Hemotek artificial feeding system (Discovery Workshops, Accrington, Lancaster, UK) for provision to laboratory reared cohorts of 50, 3- to 5-day-old, female *A. stephensi* maintained as described previously (Luckhart et al., 2003). Mosquitoes were allowed to feed on the collected rat blood for 30 min. At 1, 4, 24 and 48 h after feeding, mosquito midguts were dissected into cold PBS (Cellgro, Mediatech, Herndon, VA) on ice, homogenized by pulse sonication and flash frozen in dry ice-liquid nitrogen until analysis by TGF-β1 ELISA (R&D Systems, Minneapolis, MN). Analyses of TGF-β1 persistence and activation were replicated with 4–9 separate cohorts of 50 *A. stephensi* and blood collected from 9 rats. Mosquito midgut samples from each experimental replicate were flash frozen until analysis of endogenous latent and active TGF-β1. Values for latent/total TGF-β1 were determined in these midgut samples after acid-activation of samples with 1 N HCl, whereas endogenous active TGF-β1 levels were measured without prior acid-activation. In all cases, TGF-β1 levels are expressed as pg/midgut.

Inferences with regard to mammal-mosquito "immunological crosstalk," and, in some cases, additional experimental data, used for computational modeling of *AsNOS* and *As60A* dynamics were derived from published studies (Crampton and Luckhart, 2001a, 2001b; Lim et al., 2005; Luckhart et al., 1998, 2003, 2008; Peterson et al., 2007) with the express written consent of the publisher. Specifically, time course analyses of *AsNOS* and *As60A* expression in female *A. stephensi* were performed using data collected as described in the original publications (Luckhart et al., 2008; Crampton and Luckhart, 2001b).

Previously unpublished data are also presented herein. In particular, for analyses of the effects of AsNOS inhibition on TGF-β1-dependent *As60A* expression, active human TGF-β1 (Cell Signaling Technology, Danvers, MA), L-NAME (Sigma-Aldrich, St. Louis, MO) and D-NAME (Sigma-Aldrich) stock solutions were prepared in phosphate-buffered saline (PBS; Cellgro) and diluted directly into an artificial bloodmeal for feeding. For these experiments, the artificial bloodmeal was provided via a Hemotek feeding system and was comprised of washed human type O positive erythrocytes (Interstate Blood Bank, Memphis, TN) diluted in heat-inactivated compatible human serum. In previous work, we determined that heat-inactivation, followed by multiple freeze-thaw cycles eliminated detectable active TGF-β1 in human serum (Luckhart et al., 2003). Mosquitoes were allowed to feed on the artificial bloodmeal for 30 min. At 15 min after feeding, blood-filled midguts were dissected into PBS (Cellgro) and transferred immediately into TRI-reagent (Invitrogen, Carlsbad, CA) for RNA extraction. Total RNA from 20 mosquito midguts pooled from each treatment group were extracted as per manufacturer's instructions. These analyses of *As60A* expression were replicated with five separate cohorts of *A. stephensi*; each cohort was subdivided into four treatment groups. Relative *As60A* transcript abundance was calculated as normalized ΔC_T using a comparative cycle threshold method of analysis (User Bulletin 2, ABI Prism 7700 Sequence Detection System; Applied Biosystems, Foster City, CA) with S7 ribosomal protein gene expression as the housekeeping gene control. Primers, probes and thermal cycling conditions were described previously (Crampton and Luckhart, 2001a,b). *As60A* primers and probe included the forward primer As60AF (5′-AAAG GGACGCCGCCTATG-3′), the reverse primer As60AR (5′-CAGCTC GGCCATCAGTACACT-3′) and the Taqman® probe As60AP (6FAM-TTCGGCATTACCAACATTGAAGACGACGT-TAMRA). The *ribosomal S7* primers and probe included the forward primer S7F2 (5′-GAA GGCCTTCCAGAAGGTACAGA-3′), the reverse primer S7R2 (5′-CATC GGTTTGGGCAGAATG-3′) and the Taqman® probe S7P (VIC-AGAA GTTCTCCGGCAAGCACGTCGT-TAMRA).

2.5. Statistical analyses

Experiments were performed at least three times independently and data are presented as mean ± SE unless otherwise indicated. Statistical differences were assessed by one- or two-way analysis of variance (ANOVA) followed by a *post-hoc* test, where appropriate, using SigmaPlot 11 software (Systat Software, San Jose, CA). The level of significance for differences was set at 5%.

3. Results

3.1. Overview of experimental hypotheses and computational methods

In this study, we focused on the "immunological crosstalk" interface between the mammalian host and the anopheline

Please cite this article as: Price, I., et al., *In vivo*, *in vitro*, and *in silico* studies suggest a conserved immune module that regulates malaria parasite transmission from mammals to mosquitoes. J. Theor. Biol. (2013), http://dx.doi.org/10.1016/j.jtbi.2013.05.028

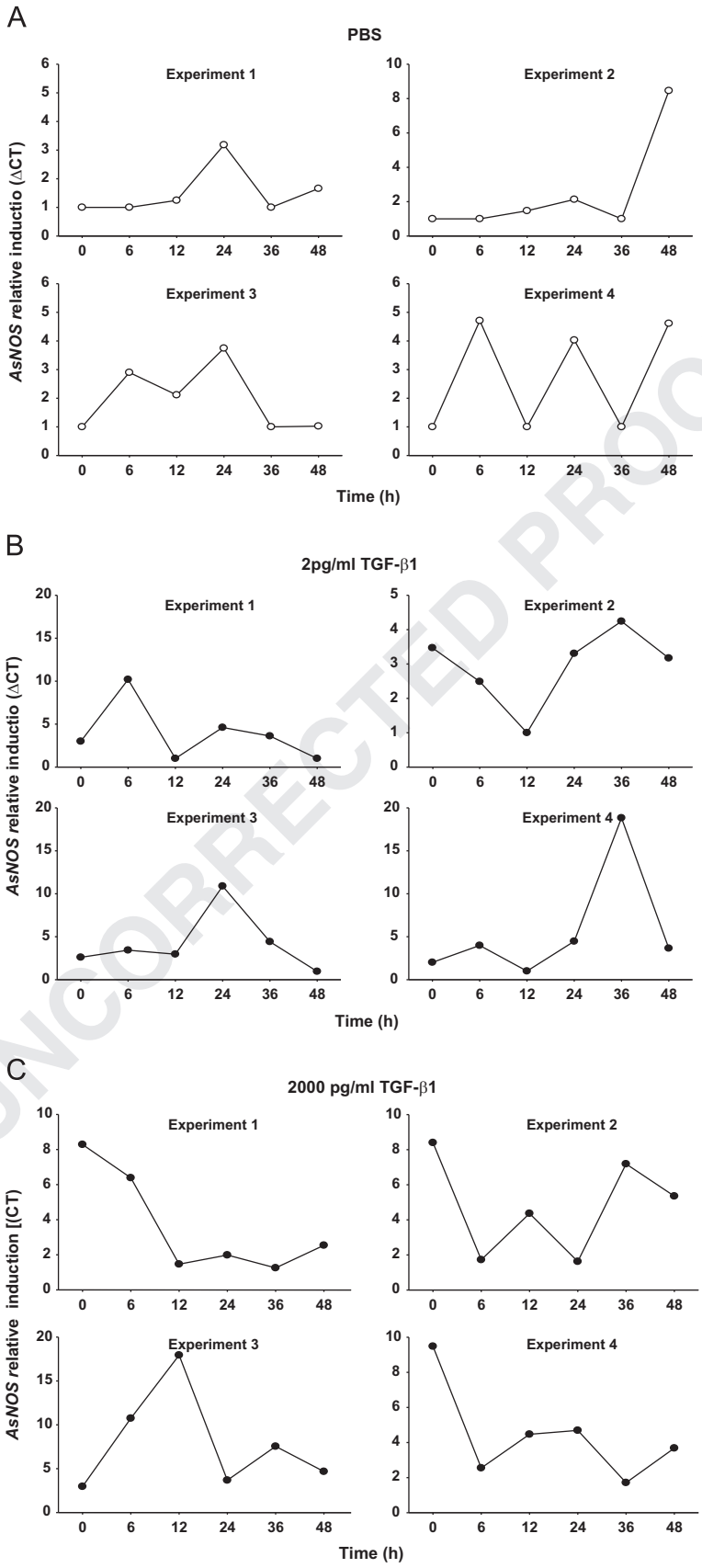

Fig. 4. Variability of experimental data across cohorts. Four separate cohorts of 50 *A. stephensi* mosquitoes were fed on artificial bloodmeals containing 0 (*Panel A*), 2 (*Panel B*), or 2000 (*Panel C*) pg/ml latent TGF-β1, and midgut *AsNOS* expression was assessed as described in Section 2. Each panel contains four sub-panels for the four experimental cohorts. This representation of the data demonstrates that qualitative features shift in time across cohorts (e.g. a single largest peak), which may be averaged out in our statistical summary (Fig. 4).

Please cite this article as: Price, I., et al., *In vivo*, *in vitro*, and *in silico* studies suggest a conserved immune module that regulates malaria parasite transmission from mammals to mosquitoes. J. Theor. Biol. (2013), http://dx.doi.org/10.1016/j.jtbi.2013.05.028

mosquito host (Fig. 1). We have suggested that the induction of *AsNOS* by ingested latent TGF-β1 leads to increased killing of *Plasmodium* parasites (Luckhart et al., 2008). Accordingly, we assumed that elevated AsNOS acts as a surrogate for parasite killing. Furthermore, we assumed that *AsNOS* mRNA expression could be linearly equated to enzymatically functional AsNOS protein, based on our prior studies (Luckhart et al., 1998). In mammalian cells, RNS modulate MAP kinase signaling (Levonen et al., 2001; Pinzar et al., 2005), and we have shown that activation of the MAP kinase signaling module MEK/ERK by reactive oxygen species leads to reduced *AsNOS* expression and impaired parasite-killing capacity in *A. stephensi* (Surachetpong et al., 2009). Accordingly, we hypothesized that AsNOS-derived RNS will activate MEK/ERK in the mosquito host as well. These interactions are depicted graphically in Fig. 1 and schematically in Fig. 2A–C (see Section 2).

Computational modeling is a powerful tool with which to unravel these complex, cross-species interactions (Akman-Anderson et al., 2007; Drexler et al., 2008; Pakpour et al., 2013). In the present studies, we utilized Boolean and ordinary differential equation (ODE) modeling in order to discern the qualitative behavior of this complex host/vector system. Boolean modeling can be used to infer emergent network behavior through relatively simple "yes/no" mechanistic rules. Mathematical models based on non-linear ODEs can be used to model biological interactions with various degrees of abstraction.

3.2. Boolean model of "immunological crosstalk" and in vitro experimental studies of MEK/ERK signaling

In modeling the mosquito-mammal "immunological crosstalk", the relevant biochemical interactions were initially depicted graphically as an influence diagram (Fig. 2A). This diagram suggested that these interactions comprise an activator-inhibitor system, with the activation mediated through the ingestion of exogenous TGF-β1. To examine the qualitative behavior of this system, we created a non-quantitative, Boolean (logical) model of the core MEK/ERK, TGF-β1, and AsNOS interactions depicted graphically in Fig. 2B (see Section 2). One qualitative prediction of this model was that upon stimulation with exogenous human TGF-β1, mosquito MEK/ERK would oscillate as long as TGF-β1 is present (Fig. 2D). To test this prediction qualitatively, immortalized anopheline 4a3B cells were stimulated with 6000 pg/ml human TGF-β1 for up to 24 h, and the levels of phosphorylated (active) ERK were assessed by immunoblotting. As seen in Fig. 2E, an apparent biphasic pattern of phospho-ERK was observed in response to TGF-β1 (black symbols), at levels higher than for unstimulated 4a3B cells (white symbols).

3.3. Boolean and ordinary differential equation models of "immunological crosstalk" predict TGF-β1-driven oscillations in AsNOS expression

The Boolean model also predicted that, like mosquito MEK/ERK signaling, *AsNOS* expression would also oscillate as long as TGF-β1 is present (Fig. 3A). Based on this prediction and the initial *in vitro* studies on TGF-β1-induced mosquito ERK activation (Fig. 2E), we hypothesized that TGF-β1, *AsNOS*, and MEK/ERK create an externally-stimulated activator-inhibitor system. Based on insights from the Boolean model and in order to gain insights into important regimes of behavior and relevant parameters of this "immunological crosstalk" system, we created a simplified mathematical model consisting of ODEs, depicted schematically in Fig. 2C (see Section 2). Like the Boolean model, ensembles of the ODE model also predicted oscillatory, or multiphasic, expression of *AsNOS* in response to ingestion of TGF-β1 (Fig. 3B–D). Further, we see evidence in the ensembles of models that, for 2000 pg/ml TGF-β1, the stable limit cycle may persist for some parameter sets, but that for other parameter sets the rise in TGF-β1 concentration leads to a disruption in the oscillations (Fig. 3D). This phenomenon can be anticipated from the one parameter bifurcation diagram for predicted steady-state *AsNOS* expression as a function of the strength of *AsNOS* induction by TGF-β1 (Fig. S1). In this analysis, we observe that if the degree to which TGF-β1 induces *AsNOS* expression is increased sufficiently, it will cross the Andronov–Hopf bifurcation from the region of stable oscillations to the region

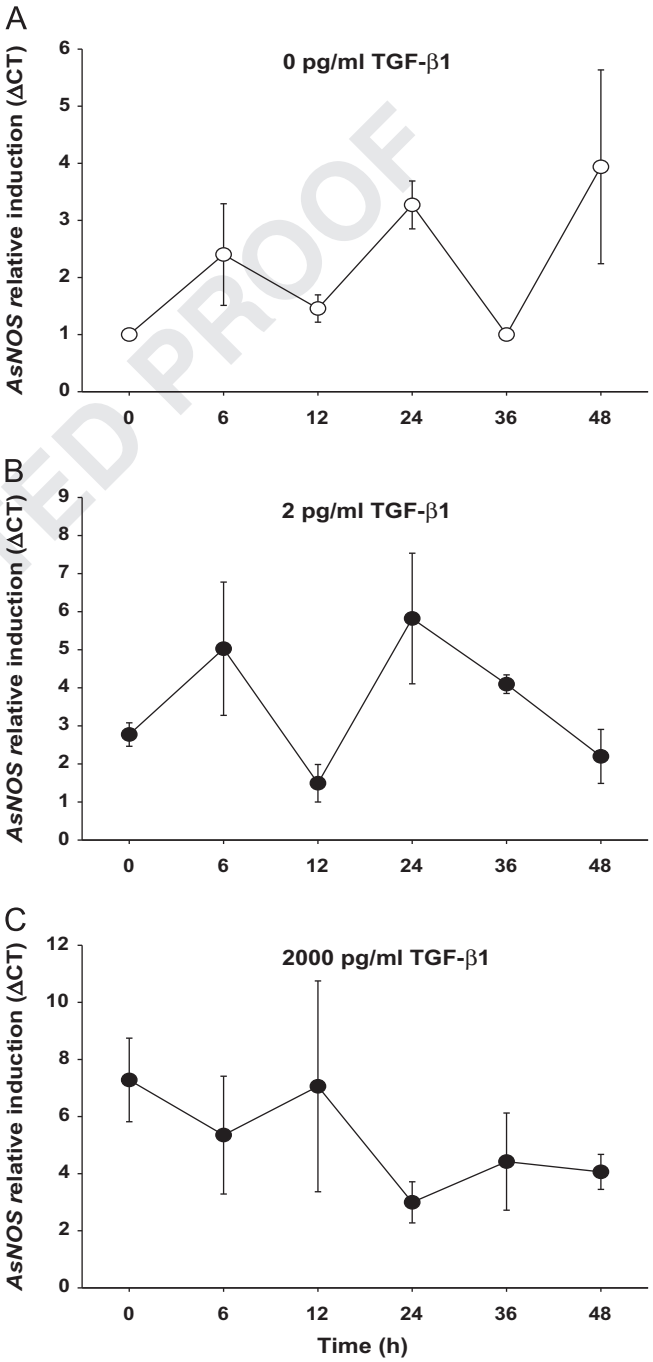

Fig. 5. Qualitative experimental validation of ODE model predictions. Separate cohorts of 50 *A. stephensi* mosquitoes were fed on artificial bloodmeals containing 0 (*Panel A*), 2 (*Panel B*), or 2000 (*Panel C*) pg/ml latent TGF-β1, and midgut *AsNOS* expression was assessed as described in Section 2. Relative expression values are shown as symbols (mean ± SEM). Data in this figure are reprinted from *Experimental Parasitology*, Volume 118, Issue 2, February 2008. Luckhart et al. Low levels of mammalian TGF-β1 are protective against malaria parasite infection, a paradox clarified in the mosquito host. Pages 290–296. Copyright 2008, with permission from Elsevier.

of stable steady-state solutions. For 2000 pg/ml TGF-β1, the final ensemble contains parameter values to both the left and the right of the bifurcation, so that from the ensemble we can expect a range of behaviors such as stable oscillations, decaying oscillations, and excitable responses.

In support of these simulations, and operating from the assumption that the lowest value of α gives a stable limit cycle, we observe a reasonable concordance to the experimental data in individual experiments, with the peaks of *AsNOS* appearing at different time points when we examine the data as replicates (Fig. 4) rather than as means $\pm$ SEM (Fig. 5).

The agglomerated data used for calibration of this ODE model are depicted in Fig. 5. In this experiment, *AsNOS* expression levels were determined following feeding of separate cohorts mosquitoes on artificial bloodmeals containing 0, 2, or 2000 pg/ml latent TGF-β1. In qualitative agreement with the ensemble of ODE models, a multiphasic expression of *AsNOS* increased from its baseline amplitude when mosquitoes were fed a bloodmeal containing 2 pg/ml TGF-β1. This behavior became more variable when the bloodmeal dose of TGF-β1 was increased to 2000 pg/ml. Moreover, Two-Way ANOVA showed an overall statistically significant difference ($P < 0.05$) among the three groups (0, 2, and 2000 pg/ml TGF-β1). Holm-Sidak *post hoc* analysis revealed a significant difference between 0 and 2000 pg/ml ($P < 0.001$) and a nearly significant difference between 2 and 2000 pg/ml ($P = 0.052$).

Importantly, we know from prior studies that cohorts of *A. stephensi* mosquitoes exhibit individual and cohort-to-cohort variability with regard to induction of *AsNOS* or phosphorylation of MAPK enzymes (Luckhart et al., 1998, 2003; Surachetpong et al., 2009, 2011). Accordingly, we hypothesized that the phase of the oscillations could differ from mosquito to mosquito within a single experimental cohort, resulting in this observed variability. If we hypothesize the presence of an ongoing oscillation of *AsNOS* in the midgut of the mosquito, then we can regard the bloodmeal as a perturbation of the oscillation coming at some phase in the cycle. Then, we sample the outputs at particular times after the bloodmeal. Since we can only get one experimental sample from each mosquito, it is very likely that the phase at which the organism is given the bloodmeal and the subsequent phases from which we sample are randomized. The bloodmeal can partially reset the oscillation, but there will still be a substantial degree of phase averaging. This will greatly suppress the ups and downs of a given cycle (Fig. 6).

To show the results of phase averaging and resetting across multiple subjects, *in silico* experiments were conducted to show the effects of phase-resetting by dose (Fig. 6). If there exists an oscillation in each individual specimen at baseline, it cannot be assumed that multiple subjects would have synchronous oscillations before receiving input. In order for an oscillation to be apparent in the data, the input to the mosquito system (the bloodmeal) must be sufficient so that there is a phase reset synchronizing the system. Unless the majority of subjects are reset to the same point in the phase, the averaged data can appear uniform. In each *in silico* experiment, 100 stochastic samples were taken from a single phase of the baseline state. As a control, no additional signal (TGF-β1) was added to the system and the average of all trajectories is given. Three different doses of TGF-β1 (2, 20, and 2000 pg/ml) were then given at time zero, assuming each of the 100 *in silico* subjects starts at a randomly chosen point of the oscillation. Twenty pg/ml was chosen as an intermediate contrast. The control (solid line) shows a nearly flat line, indicating that without additional input, we may not expect to see oscillations in the output data. For 2 pg/ml (dotted line), moderate up-down behavior is seen, indicating some phase-resetting from a bloodmeal. For 20 pg/ml (dashed line), the output becomes nearly synchronous, suggesting full phase re-setting. For

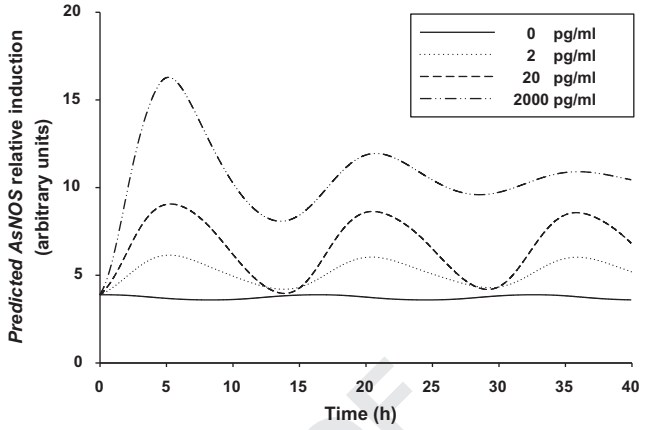

Fig. 6. Suppression of *AsNOS* oscillations through averaging over phases. Averaged plots of the N (*AsNOS*) variable in our model with the initial conditions stochastically varied across the phase of the oscillation. A control curve and three experimental curves (2, 20, and 2000 pg/ml) were simulated 100 times each with initial conditions stochastically drawn from one period of the unstimulated system. The control curve (solid) shows that in the absence of a phase re-setting event, data collection approaches a uniform average across the experimental time frame. Increasing doses of TGF-β1 induce increased amplitude and synchronicity; the 2 pg/ml dose (dotted) shows some increased synchronicity beyond the control, while 20 pg/ml (dashed) shows substantial synchronous peaks. The 2000 pg/ml dose (dash double dot) shows large initial synchronicity, but the loss of stable oscillations increases the variability for later times.

2000 pg/ml (dash double-dotted line), the output continues to be synchronous, but the true oscillations are lost to the Andronov–Hopf bifurcation (*Supplementary material*, Fig. S1). In total, assuming an oscillatory system, we might suppose that low doses of TGF-B1 would cause some phase re-setting and that the magnitude of the phase re-setting increases with dose. However, as the dose increases, we may not see true oscillations due to the Andronov–Hopf bifurcation.

3.4. Principal component analysis and bifurcation analyses of ODE model of "immunological crosstalk"

We next carried out a principal component analysis in order to determine the relative impact of changes in strengths of interactions among the biological components in our mathematical model (Table 1). From this analysis, we determined two of the universal parameters to which the system is most sensitive, as well as individual parameters to which independent experiments are sensitive. The system, as a whole, is sensitive to the value of the exponent for the competitive inhibitor, q, and to the decay rate of MEK/ERK. μ_x. On an individual experiment level, we find that simulations of the response to 2 pg/ml TGF-β1 are sensitive to the initial value of phospho-ERK, and that simulations of the response to 2000 pg/ml TGF-β1 are sensitive to the value of α.

Based on the principal component analysis, we found that a key parameter driving the multiphasic behavior in the ODE model was μ_x, the rate of decay for the inhibitor of the system. On a systematic basis, we then investigated the relationship between the rate of decay and the initial concentration of TGF-β1; this was done via bifurcation analysis in two parameters (shown in *Supplementary materials*, Fig. S2). We found from this analysis that the rate of decay for the inhibitor plays a role in the global dynamics of the system. For very fast decay of the inhibitor (increase in the *y*-axis), the system cannot sustain any significant non-linear behaviors, e.g. oscillations. As the decay slows, the bifurcation analysis shows a fold point, below which non-linear behaviors may occur depending on the size of the bolus, represented by α. Fig. S2 shows us that the system is capable of supporting either non-linear behavior of AsNOS levels in the midgut or a gravitation of AsNOS to a baseline

Please cite this article as: Price, I., et al., *In vivo*, *in vitro*, and *in silico* studies suggest a conserved immune module that regulates malaria parasite transmission from mammals to mosquitoes. J. Theor. Biol. (2013), http://dx.doi.org/10.1016/j.jtbi.2013.05.028

state. Further, important in determining the response in the midgut is the relationship between the rate of inhibitor decay and the magnitude of the initial TGF-β1 bolus.

3.5. *In silico prediction of a requirement for induction of a mosquito homolog of TGF-β1 in order to drive multiphasic expression of AsNOS*

All of the above results are predicated on the assumption that the direct effect of exogenous TGF-β1 on the system persists for the entire time frame of the experiment. In previous studies, we had indeed observed that latent mouse TGF-β1 was activated to nearly 100% within 1 h after feeding and that active mouse TGF-β1 persisted through at least 48 h in the *A. stephensi* midgut (Luckhart et al., 2003). In contrast, our data here suggested that not all mammalian hosts are equivalent: ingested latent rat TGF-β1 was not fully activated within 1 h after feeding and neither latent nor active TGF-β1 was detectable after 24 h (Fig. 7). These differences suggested that a conservative model would necessarily assume that, following ingestion from some mammalian hosts, both active (Fig. 7A) and latent (Fig. 7B) mammalian TGF-β1 are depleted from the mosquito midgut with an apparent half-life of 3–5 h. Therefore, exogenous, mammalian host-derived TGF-β1 may not persist as the direct stimulus for the oscillatory behavior we hypothesize, and yet the ODE model clearly indicates at minimum an indirect effect correlated to the dose of TGF-β1 introduced into the midgut.

In order to address this paradox, we hypothesized that an endogenous, mosquito TGF-β1-like cytokine exists within the midgut that is induced by exogenous and perhaps short-lived mammalian TGF-β1, and whose expression persists within the experimental time-frame of the above studies. This aspect of the model led us to investigate the *A. stephensi* TGF-β homolog As60A (Crampton and Luckhart, 2001a, 2001b) as a candidate, leading to the revised schematics represented in Fig. 8A–B. A corollary to this hypothesis is that the expression of *As60A* should exhibit a multiphasic behavior over time in the absence of stimuli beyond the TGF-β1 found in the mouse bloodmeal. Fig. 8C, originally published in Crampton and Luckhart (2001b), shows the variability in these data, which did not appear to vary linearly nor to merely decay.

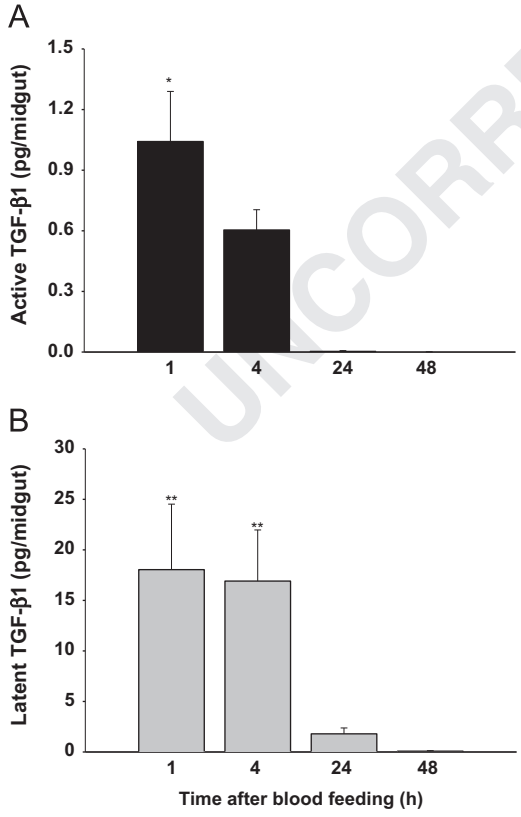

Fig. 7. Experimental studies suggest a decay of ingested rat TGF-β1 in the *A. stephensi* midgut by 24 h. *A. stephensi* mosquitoes were allowed to feed on collected rat blood for 30 min. At 1–48 h as indicated, the levels of active (*Panel A*) and latent (*Panel B*) TGF-β1 in dissected midguts were determined as described in Section 2. Results represent the mean ± SEM from 9 separate cohorts for 1 and 4 h, and 4 separate cohorts for 24 and 48 h. (Panel **A**: $^{*}P < 0.05$ vs. 24 and 48 h (overall significance $P < 0.001$); Panel **B**: $^{**}P < 0.05$ vs. 48 h (overall significance $P = 0.002$); analyzed by one-way ANOVA followed by Dunn's Method).

3.6. *In silico prediction of a requirement for AsNOS for the TGF-β1-dependent induction of mosquito As60A*

Our ODE model simulations led to the further hypothesis that the TGF-β1-stimulated induction of *As60A* was dependent on endogenous NO. In contrast, we observed that *A. stephensi* mosquitoes fed on artificial bloodmeals containing TGF-β1 along with the NOS inhibitor L-NAME (but not the inactive enantiomer, D-NAME) exhibited increased induction of *As60A* expression in the midgut (Fig. 8D). This result appeared initially to contradict the hypothesis raised by our ODE model. However, in a prior study (Luckhart et al., 2008), an examination of the expression of *AsNOS* in the same midgut tissue showed that provision of L-NAME, but not D-NAME, was associated with an increase in *AsNOS*. This finding suggests that L-NAME, by suppressing NOS catalytic activity, relieves an NO-dependent negative feedback that, in turn, leads to increased induction of *As60A*.

4. Discussion

4.1. *Interactions among host and vector factors during bloodfeeding drive complex biology that can kill malaria parasites*

In *Anopheles* mosquitoes, the malaria parasite *Plasmodium* is released into the saliva during bloodfeeding. Bloodfeeding results in crosstalk between the mammalian and mosquito immune systems at the midgut epithelium as well as in the mosquito body (Akman-Anderson et al., 2007; Pakpour et al., 2013). Our overarching goal is to understand how evolutionarily conserved, shared mechanisms of immune modulation in mosquitoes and mammals function to minimize *P. falciparum* infection (Luckhart et al., 1998, 2003, 2008).

In mice and humans, the induction of iNOS is a primary defense mechanism against *Plasmodium* (Clark et al., 2004; Nahrevanian, 2006), one that is regulated negatively by the cytokine TGF-β1 (Vodovotz, 1997). Furthermore, the MAPKs (ERK, JNK, and p38) have been implicated in the mammalian innate immune response to malaria infection (Zhu et al., 2005; Lu et al., 2006; Patel et al., 2007). In mammals, iNOS-derived RNS can lead to the activation of endogenous latent TGF-β1 (Vodovotz et al., 1999, 2004; Luckhart et al., 2008). Similarly, the *A. stephensi* iNOS homolog AsNOS acts to limit *Plasmodium* development (Luckhart et al., 1998, 2003; Lim et al., 2005; Peterson et al., 2007). Mammalian TGF-β1 circulates at high levels – though mostly in the latent form (Flaumenhaft et al., 1993; Annes et al., 2003; Zamora and Vodovotz, 2005) – and can be activated by endogenous RNS in the mosquito midgut, can regulate mosquito signaling, and ultimately can reduce the *Plasmodium* burden in *A. stephensi* (Luckhart et al., 2003, 2008).

In order to understand how AsNOS and TGF-β1 function to regulate parasite development, we have examined the signaling pathways by which this immunoregulatory inter-species crosstalk occurs, guided by advances in the field of mammalian immunity and inflammation. In mammals, the MAPK pathways are regulated

Please cite this article as: Price, I., et al., *In vivo*, *in vitro*, and *in silico* studies suggest a conserved immune module that regulates malaria parasite transmission from mammals to mosquitoes. J. Theor. Biol. (2013), http://dx.doi.org/10.1016/j.jtbi.2013.05.028

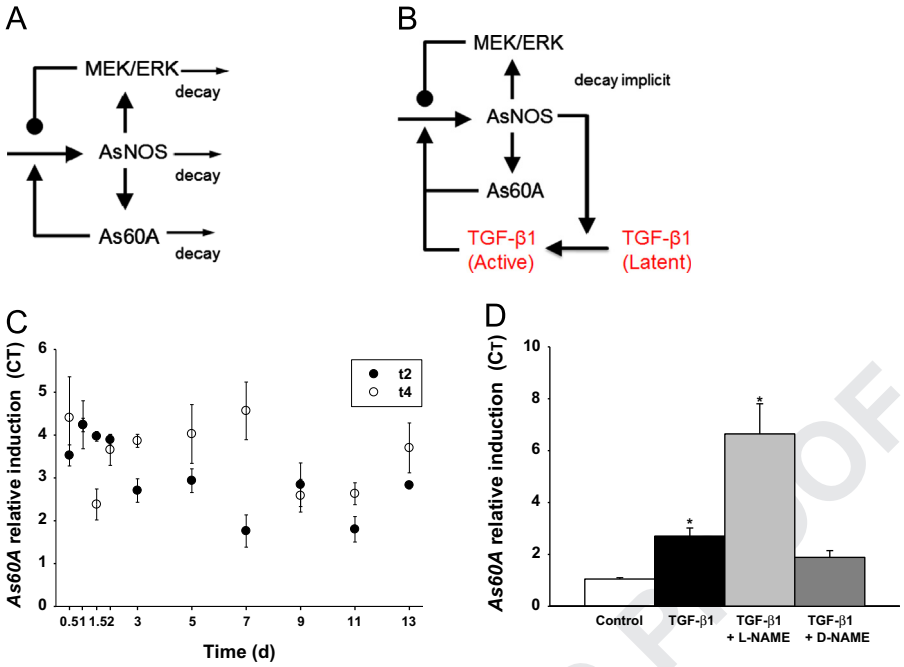

Fig. 8. Computational modeling suggests, and *in vivo* studies support, a role for TGF-β1 and NO in inducing *As60A*. *Panel A*: The hypothesized interactions among mammalian TGF-β1, mosquito AsNOS, and mosquito MEK/ERK signaling described in Fig. 1A–B were expanded to include a hypothesized induction of mosquito *As60A* by ingested mammalian TGF-β1. *Panel B*: Simplification of the schematic depicted in *Panel A*. Red text indicates host-derived molecule, and black text indicates mosquito-derived molecules and processes. *Panel C*: Two separate cohorts of *A. stephensi* mosquitoes (t2 and t4) were fed on ICR mice, and midgut *As60A* expression determined at various time points after bloodfeeding as described in Section 2. Expression values are mean ± SEM of 20 individual mosquitoes. *Panel D*: Five cohorts of *A. stephensi* mosquitoes were fed on artificial bloodmeals containing PBS (control), 2000 pg/ml TGF-β1, or 2000 pg/ml pg/ml TGF-β1 along with either 1 mg/ml L-NAME or 1mg/ml D-NAME, as indicated. *As60A* expression levels were determined as described in the *Methods* ($n=5$, $^*P<0.05$ vs. Control, analyzed by Kruskal–Wallis one-way ANOVA on Ranks followed by Tukey test). Data in *Panel C* are reprinted from *Infection Genetics and Evolution*, Volume 1, Issue 2, December 2001. Crampton and Luckhart. The role of As60A, a TGF-β homolog, in *Anopheles stephensi* innate immunity and defense against *Plasmodium* infection. Pages 131–141. Copyright 2001, with permission from Elsevier. (For interpretation of the references to color in this figure legend, the reader is referred to the web version of this article.)

by both TGF-β1 (Massague, 2000) and RNS (Levonen et al., 2001). TGF-β1 signaling in anopheline cells is regulated by redox chemistry, involves differential activation of the homologs of the MAPKs and regulates TGF-β1 dose-dependent effects on *AsNOS* and malaria parasite burdens (Surachetpong et al., 2009) (Fig. 1).

Receptor dynamics play a prominent role in the signal-response pathways of the TGF-β superfamily (Di Guglielmo et al., 2003; Mitchell et al., 2004), and modeling of *in vitro* data has suggested various trafficking patterns based on the mix of transient and permanent contributions to signaling (Vilar and Saiz, 2011). The explicit effects of receptor dynamics on TGF-β1-mediated crosstalk to anopheline cells could affect AsNOS expression on the experimentally-probed timescale but are beyond the scope of the current model.

4.2. Insights from computational modeling of host-vector "immunological crosstalk" in malaria

Herein, we attempted to synthesize these data and address key aspects of the complexity of this biology – in part qualitatively and in part quantitatively – in order to predict key aspects of the aggregate behavior of this cross-species interaction, through a process of combined mathematical modeling and experimentation. These studies led to several mutually-affirming, but not fully verified, hypotheses: (1) that the expression of mosquito *AsNOS* exhibits oscillatory or quasi-oscillatory behavior at baseline; (2) that this multiphasic expression is augmented by ingested mammalian TGF-β1 but may require the long-term presence of a TGF-β1-like influence; (3) that, since mammalian TGF-β1 can be degraded in the midgut within hours, this TGF-β1-like influence is possibly carried out by mosquito As60A; and (4) that the mammalian TGF-β1-induced activation of mosquito MEK/ERK signaling exhibits a multiphasic behavior, as well as being induced by AsNOS-derived RNS and suppressing the further induction of *AsNOS* by TGF-β1/As60A.

4.3. Multiphasic expression of key "immunological crosstalk" components occurs in biological systems other than malaria

The central feature of this system, then, is the predicted multiphasic behavior of AsNOS and MEK/ERK signaling, driven initially by exogenous TGF-β1 and maintained by endogenous As60A. This behavior is consistent with that observed in mammals, in which MAPK activation exhibits oscillating behavior (Araujo et al., 2001; Chickarmane et al., 2007; Weber et al., 2010). Likewise, there are examples in mammalian systems of NO-driven oscillations in diverse biological processes (Keef et al., 1997; Fujie et al., 2005), of cyclical patterns in iNOS expression (Porras et al., 2006), and of oscillatory platelet and leukocyte counts driven by TGF-β1 negative feedback (Hirayama et al., 2003). Indeed, many biological networks that exhibit positive and negative feedback, such as the one under study here, oscillate (Novak and Tyson, 2008). Importantly, studies of the genome of *P. falciparum* also suggest genome-level oscillations in the parasite (Bozdech et al., 2003), raising the intriguing possibility that the pathogen-vector-host system as has evolved response complementarity to these multiphasic dynamics.

Based on the two-dimensional mathematical model we created based on the mechanistic interactions of the system, there exist two analytically distinct behaviors for *AsNOS*; oscillation and attraction to fixed point. These two behaviors depend on parameter choice, and we suggest the existence of an Andronov–Hopf bifurcation as TGF-β1 increases based on our simulations. Given the experimental system used, in which data are derived not from cohorts of individual mosquitoes that feed on blood over a 30-min

Please cite this article as: Price, I., et al., *In vivo*, *in vitro*, and *in silico* studies suggest a conserved immune module that regulates malaria parasite transmission from mammals to mosquitoes. J. Theor. Biol. (2013), http://dx.doi.org/10.1016/j.jtbi.2013.05.028

time frame, it is possible that some *A. stephensi* mosquitoes exhibit multiphasic *AsNOS* expression and some do not; validating this hypothesis will require additional studies.

4.4. *In silico* prediction of the need for sustained, TGF-β1-driven multiphasic expression of AsNOS via mosquito As60A

In order to maintain this multiphasic behavior of *AsNOS*, our model hypothesized the persistent presence of a TGF-β1-like influence that we inferred, at least in some settings, to be dependent on the mosquito TGF-β homolog As60A. Moreover, this induction was predicted to occur via the induction of *AsNOS*. In support of these predictions, we indeed found that TGF-β1 induces *As60A* and that this induction is negatively regulated by NO. Indeed, the action of TGF-β1 in the context of parasite infection may be potentiated by the *A. stephensi* TGF-β ortholog As60A. *As60A* expression is induced in the mosquito midgut epithelium in response to *Plasmodium* infection—this response appears to depend on parasite load and to be correlated with periods of parasite motility and growth (Crampton and Luckhart, 2001a, 2001b). Our data suggest that when mosquitoes are fed on live mice, latent TGF-β1 is activated completely within 1 h and the active TGF-β1 is detectable out to 48 h, with a half-life of approximately 24 h (Luckhart et al., 2003). In contrast, latent rat TGF-β1 is activated to a much lesser maximal extent within 1 h, and both active and latent TGF-β1 appear to persist for approximately 4 h. It is unclear at this point if these differences are due to feeding on a live host versus collected blood from a live host, or whether the difference is due to the species (mouse or rat) from which the blood was derived. These different results suggest that ingested TGF-β1 could persist for a sufficient time to drive the multiphasic expression of *AsNOS* directly, but that even if TGF-β1 levels do not persist, *As60A* induced by TGF-β1 could substitute in driving the multiphasic expression of *AsNOS*.

Given that TGF-β1 controls parasite infection in the mosquito host via synthesis of toxic RNS (Luckhart et al., 2008), we might presume that the induction of AsNOS by As60A performs the same function in a very straightforward way. However, 60A signaling in the fruit fly *Drosophila melanogaster* is also activated to restore energy homeostasis through upregulated synthesis of insulin-like peptides (Ballard et al., 2010), much in the same way that elevated insulin stimulates increased energy stores in humans. We have recently shown that when energy homeostasis downstream of insulin signaling is dysregulated in *A. stephensi*, the resultant high-level synthesis of RNS completely inhibits *P. falciparum* development (Luckhart et al., 2013). Hence, future studies and accompanying modeling will test the hypothesis that As60A in fact participates in a dynamic signaling network that regulates "metabolic inflammation" to control parasite development in the mosquito.

4.5. *Limitations of the current study*

There are several limitations to our study, which stem from the relatively simple mathematical models created in an attempt to explain the experimental data. As discussed above, our data from *A. stephensi* may be insufficient to fully prove a multiphasic behavior of *AsNOS*, *As60A*, and *A. stephensi* MEK/ERK signaling. Using standard statistical tools (polynomial regression), we observed that the dynamics of phospho-ERK activation *in vitro*, as well as *As60A* expression *in vivo*, could be fit fairly well with 4th- and 5th-order polynomials, but poorly with a linear regression model (data not shown). In the case of TGF-β1-induced *AsNOS* expression *in vivo*, however, low r^2 values were obtained for 1st–5th-order polynomial regressions (data not shown), suggesting that this biological system is more complex and lacking interactions not included in our simple Boolean and ODE models. We would argue that this is the value of multi-objective fitting (as performed in order to calibrate the ODE model we created herein), in that multiple data sets can indirectly aid in creating a full picture of what happens during the entire time course. For example, the ensemble for 2000 pg/ml would show a much tighter fit to the data without the need for the system to also fit to the data for PBS and 2 pg/ml TGF-β1; instead, our model ensemble shows a robust combination of oscillations and decaying oscillations.

Nonetheless, the present study leads to the hypothesis that there exist time points for which the value of *AsNOS* is high and that were not captured in the data collection. From a technical point of view, as mentioned above, we note that each *in vivo A. stephensi* study consists of a 30-min feeding period to a cohort of mosquitoes, during which time mosquitoes within a given experimental cohort are feeding at variable rates to various degrees on whatever experimental substance is introduced into their artificial bloodmeal. While we have tried to model this variability through the use of ensembles of models, this unavoidable logistical necessity adds both difficulty and variability to our ability to obtain data at the exact time points stipulated by computational simulations.

Given the nature of the individual replicates, our assertion is that the data are best represented by a non-linear model. Taken together, the data shown in Fig. 4A–C on TGF-β1-induced expression of *AsNOS* exhibit several properties that a linear model does not reproduce. On inspection of the individual datasets (Fig. 4), *AsNOS* expression is neither monotonically increasing nor decreasing over the experimental time frame for any of the replicates. Furthermore, several experimental replicates show a primary elevation in *AsNOS* expression as well as a secondary elevation, with inconsistent timing among replicates. While such behavior does not prove conclusively the existence of multiphasic expression, these features which are endemic in the data are not well-represented by a linear model. The use of oscillations in the model allows it to reproduce sudden increases and decreases in *AsNOS* expression as seen in the individual trajectories, which would not be represented in a linear model.

The results of our *in silico* models, fit to the data, suggest oscillations as the non-linear behavior that describes the observed phenomena most accurately in a deterministic setting. This does not preclude alternative models based on decaying oscillations, stochastic models, or other non-linear models. However, given the data and model, we assert that our mathematical model predicts a likelihood of oscillatory behavior only in the experimental timeframe.

5. Conclusions

Our ultimate goal is to understand the mosquito as not simply a vector of malaria parasites, but as a potential tool to limit the spread of this disease-causing parasite. The model described herein provides a first systems-level analysis of the immune processes in the mosquito midgut. It predicts that an endogenous version of the same cytokine may be necessary to drive the multiphasic expression of *AsNOS*. The impact of this crosstalk on parasite transmission is likely to be significant, since recent studies suggest that oscillations are a necessary outcome of biological tradeoffs (Chandra et al., 2011). From this point of view, *Anopheles* mosquitoes may have evolved to balance effective parasite killing mediated by RNS against the damage that prolonged elevations of such species may cause to the mosquito itself. Of note, *A. stephensi* has only a single *NOS* gene, though multiple transcripts are generated from this gene, presumably via alternative splicing (Luckhart et al., 1998), and some of these alternate forms may serve to mediate normal mosquito

Please cite this article as: Price, I., et al., *In vivo*, *in vitro*, and *in silico* studies suggest a conserved immune module that regulates malaria parasite transmission from mammals to mosquitoes. J. Theor. Biol. (2013), http://dx.doi.org/10.1016/j.jtbi.2013.05.028

physiology. Thus, the mosquito may balance relatively brief elevations of high-level expression of *AsNOS* to kill *Plasmodium*, and then restore the levels of RNS to those necessary to drive normal physiological processes. Indeed, *AsNOS* can be induced quite rapidly (within 30 min) upon bloodfeeding (Luckhart et al., 2008). Our simulations suggest that the inherent oscillatory behavior of *AsNOS* would allow for a very rapid upregulation of this enzyme, which presumably would benefit the mosquito host in combating *Plasmodium* infection. However, there are tradeoffs with regard to overexuberant capacity to kill the parasite: multiple studies have suggested that parasite killing capacity comes at a fitness cost to the mosquito, typically observed as reduced lifespan (Hurd et al., 2005; Voordouw et al., 2008; Corby-Harris et al., 2010; Luckhart et al., 2013). We suggest that computational modeling may highlight key mechanisms and drivers of such tradeoffs that may be exploited to reduce parasite transmission while taking into consideration the complex ecology of malaria.

Acknowledgments

This work was supported by NIAID grants RO1 AI050663 and RO1 AI080799 (BE, RZ, BW, NA, GC, JF, SL, YV).

Appendix A. Supporting information

Supplementary data associated with this article can be found in the online version at http://dx.doi.org/10.1016/j.jtbi.2013.05.028.

References

Akman-Anderson, L., Vodovotz, Y., Zamora, R., Luckhart, S., 2007. Bloodfeeding as an interface of mammalian and arthropod immunity. In: Beckage, N (Ed.), Insect Immunology. Elsevier, Elsevier, pp. 149–177, pp. 149-177.

Albert, I., Thakar, J., Li, S., Zhang, R., Albert, R., 2008. Boolean network simulations for life scientists. Source Code Biol. Med. 3, 16.

Annes, J.P., Munger, J.S., Rifkin, D.B., 2003. Making sense of latent TGFbeta activation. J. Cell Sci. 116, 217–224.

Anstey, N.M., Weinberg, J.B., Hassanali, M.Y., Mwaikambo, E.D., Manyenga, D., Misukonis, M.A., Arnelle, D.R., Hollis, D., McDonald, M.I., Granger, D.L., 1996. Nitric oxide in Tanzanian children with malaria: Inverse relationship between malaria severity and nitric oxide production/nitric oxide synthase type 2 expression. J. Exp. Med. 184, 557–567.

Araujo, E.G., Bianchi, C., Faro, R., Sellke, F.W., 2001. Oscillation in the activities of MEK/ERK1/2 during cardiopulmonary bypass in pigs. Surgery 130, 182–191.

Attisano, L., Lee-Hoeflich, S.T., 2001. The smads. Genome Biol. 2, REVIEWS3010.

Ballard, S.L., Jarolimova, J., Wharton, K.A., 2010. Gbb/BMP signaling is required to maintain energy homeostasis in Drosophila. Dev. Biol. 337, 375–385.

Bertsekas, D., 1995. Non-linear Programming. Athena Scientific, Belmont, MA.

Blanco, F.J., Geng, Y., Lotz, M., 1995. Differentiation-dependent effects of IL-1 and TGF-β on human articular chondrocyte proliferation are related to inducible nitric oxide synthase expression. J. Immunol. 154, 4018–4026.

Bozdech, Z., Llinas, M., Pulliam, B.L., Wong, E.D., Zhu, J., DeRisi, J.L., 2003. The transcriptome of the intraerythrocytic developmental cycle of *Plasmodium falciparum*. PLoS Biol. 1, E5.

Chandra, F.A., Buzi, G., Doyle, J.C., 2011. Glycolytic oscillations and limits on robust efficiency. Science 333, 187–192.

Chickarmane, V., Kholodenko, B.N., Sauro, H.M., 2007. Oscillatory dynamics arising from competitive inhibition and multisite phosphorylation. J. Theor. Biol. 244, 68–76.

Clark, I.A., Alleva, L.M., Mills, A.C., Cowden, W.B., 2004. Pathogenesis of malaria and clinically similar conditions. Clin. Microbiol. Rev. 17, 509–539.

Corby-Harris, V., Drexler, A., Watkins de Jong, L., Antonova, Y., Pakpour, N., Ziegler, R., Ramberg, F., Lewis, E.E., Brown, J.M., Luckhart, S., Riehle, M.A., 2010. Activation of Akt signaling reduces the prevalence and intensity of malaria parasite infection and lifespan in *Anopheles stephensi* mosquitoes. PLoS Pathog., 6; p. e1001003.

Crampton, A.L., Luckhart, S., 2001a. Isolation and characterization of As60A, a transforming growth factor-β gene, from the malaria vector *Anopheles stephensi*. Cytokine 13, 65–74.

Crampton, A.L., Luckhart, S., 2001b. The role of As60A, a TGF-β homolog, in Anophelesstephensi innate immunity and defense against Plasmodium infection. Infect. Genet. Evol. 1, 131–141.

Di Guglielmo, G.M., Le, R.C., Goodfellow, A.F., Wrana, J.L., 2003. Distinct endocytic pathways regulate TGF-beta receptor signalling and turnover. Nat. Cell Biol. 5, 410–421.

Dodoo, D., Omer, F.M., Todd, J., Akanmori, B.D., Koram, K.A., Riley, E.M., 2002. Absolute levels and ratios of proinflammatory and anti-inflammatory cytokine production *in vitro* predict clinical immunity to *Plasmodium falciparum* malaria. J. Infect. Dis. 185, 971–979.

Doedel, E.J., 1981. AUTO: A program for the automatic bifurcation analysis of autonomous systems. In: Tenth Manitoba Conference on Numerical Mathematics and Computing. Congressus Numerantium 30, 265–284. 4-1-1981. Winnipeg, Canada. 9-1-1980.

Drexler, A.L., Vodovotz, Y., Luckhart, S., 2008. *Plasmodium* development in the mosquito: biology bottlenecks and opportunities for mathematical modeling. Trends Parasitol. 24, 333–336.

Dunachie, S.J., Berthoud, T., Keating, S.M., Hill, A.V., Fletcher, H.A., 2010. MIG and the regulatory cytokines IL-10 and TGF-β1 correlate with malaria vaccine immunogenicity and efficacy. PLoS ONE 5, e12557.

Edelstein-Keshet, L., 2005. Mathematical Models in Biology. Society for Industrial and Applied Mathematics, Philadelphia.

Ermentrout, B., 2002. Simulating, Analyzing, and Animating Dynamical Systems a Guide to XPPAUT for Researchers and Students. Society for Industrial and Applied Mathematics, Philadelphia.

Flaumenhaft, R., Kojima, S., Abe, M., Rifkin, D.B., 1993. Activation of latent transforming growth factor β. Adv. Pharmacol. 24, 51–76.

Fujie, S., Yamamoto, T., Murakami, J., Hatakeyama, D., Shiga, H., Suzuki, N., Ito, E., 2005. Nitric oxide synthase and soluble guanylyl cyclase underlying the modulation of electrical oscillations in a central olfactory organ. J. Neurobiol. 62, 14–30.

Gilbert, R.S., Herschmann, H.R., 1993. Transforming growth factor beta differentially modulates the inducible nitric oxide synthase gene in distinct cell types. Biochem. Biophys. Res. Commun. 195, 380–384.

Goureau, O., Lepoivre, M., Becquet, F., Courtois, Y., 1993. Differential regulation of inducible nitric oxide synthase by fibroblast growth factors and transforming growth factor β in bovine retinal epithelial cells: inverse correlation with cellular proliferation. Proc. Nat. Acad. Sci. U.S.A. 90, 4276–4280.

Hirayama, Y., Sakamaki, S., Tsuji, Y., Matsunaga, T., Niitsu, Y., 2003. Cyclic platelet and leukocyte count oscillation in chronic myelocytic leukemia regulated by the negative feedback of transforming growth factor beta. Int. J. Hematol. 77, 71–74.

Hurd, H., Taylor, P.J., Adams, D., Underhill, A., Eggleston, P., 2005. Evaluating the costs of mosquito resistance to malaria parasites. Evolution 59, 2560–2572.

Keef, K.D., Murray, D.C., Sanders, K.M., Smith, T.K., 1997. Basal release of nitric oxide induces an oscillatory motor pattern in canine colon. J. Physiol. 499 (Pt 3), 773–786.

Kim, S.J., Glick, A., Sporn, M.B., Roberts, A.B., 1989a. Characterization of the promoter region of the human transforming growth factor-β1 gene. J. Biol. Chem. 264, 402.

Kim, S.J., Jeang, K.T., Glick, A.B., Sporn, M.B., Roberts, A.B., 1989b. Promoter sequences of the human transforming growth factor-β1 gene responsive to transforming growth factor-β1 autoinduction. J. Biol. Chem. 264, 7041.

Kim, S.-J., Denhez, F., Kim, K.Y., Holt, J.T., Sporn, M.B., Roberts, A.B., 1989c. Activation of the second promoter of the transforming growth factor-Beta1 gene by transforming growth factor-Beta1 and phorbol ester occurs through the same target sequences. J. Biol. Chem. 264, 19373–19378.

Kolch, W., 2000. Meaningful relationships: the regulation of the Ras/Raf/MEK/ERK pathway by protein interactions. Biochem. J. 351 (Pt 2), 289–305.

Kyriakis, J.M., Avruch, J., 2012. Mammalian MAPK signal transduction pathways activated by stress and inflammation: a 10-year update. Physiol. Rev. 92, 689–737.

Levonen, A.L., Patel, R.P., Brookes, P., Go, Y.M., Jo, H., Parthasarathy, S., Anderson, P. G., Darley-Usmar, V.M., 2001. Mechanisms of cell signaling by nitric oxide and peroxynitrite: from mitochondria to MAP kinases. Antioxid. Redox Signal. 3, 215–229.

Lim, J., Gowda, D.C., Krishnegowda, G., Luckhart, S., 2005. Induction of nitric oxide synthase in *Anopheles stephensi* by *Plasmodium falciparum*: mechanism of signaling and the role of parasite glycosylphosphatidylinositols. Infect. Immun 73, 2778–2789.

Lu, Z., Serghides, L., Patel, S.N., Degousee, N., Rubin, B.B., Krishnegowda, G., Gowda, D.C., Karin, M., Kain, K.C., 2006. Disruption of JNK2 decreases the cytokine response to *Plasmodium falciparum* glycosylphosphatidylinositol *in vitro* and confers protection in a cerebral malaria model. J. Immunol. 177, 6344–6352.

Luckhart, S., Crampton, A.L., Zamora, R., Lieber, M.J., Dos Santos, P.C., Peterson, T.M. L., Emmith, N., Lim, J., Wink, D.A., Vodovotz, Y., 2003. Mammalian transforming growth factor-β1 activated after ingestion by *Anophelesstephensi* modulates mosquito immunity. Infect. Immun. 71, 3000–3009.

Luckhart, S., Giulivi, C., Drexler, A.L., Antonova-Koch, Y., Sakaguchi, D., Napoli, E., Wong, S., Price, M.S., Eigenheer, R., Phinney, B.S., Pakpour, N., Pietri, J.E., Cheung, K., Georgis, M., Riehle, M., 2013. Sustained activation of Akt elicits mitochondrial dysfunction to block *Plasmodium falciparum* Infection in the mosquito host. PLoS Pathog., In Press.

Luckhart, S., Lieber, M.J., Singh, N., Zamora, R., Vodovotz, Y., 2008. Low levels of mammalian TGF-β1 are protective against malaria parasite infection, a paradox clarified in the mosquito host. Exp. Parasitol. 118, 290–296.

Luckhart, S., Vodovotz, Y., Cui, L., Rosenberg, R., 1998. The mosquito *Anopheles stephensi* limits malaria parasite development with inducible synthesis of nitric oxide. Proc. Nat. Acad. Sci. U.S.A. 95, 5700–5705.

Please cite this article as: Price, I., et al., *In vivo*, *in vitro*, and *in silico* studies suggest a conserved immune module that regulates malaria parasite transmission from mammals to mosquitoes. J. Theor. Biol. (2013), http://dx.doi.org/10.1016/j.jtbi.2013.05.028

Massague, J., 2000. How cells read TGF-beta signals. Nat. Rev. Mol. Cell Biol. 1, 169–178.

Mellouk, S., Hoffman, S.L., Liu, Z.Z., Billiar, l.d.e.,V.,T.R., Nussler, A.K., 1994. Nitric oxide-mediated antiplasmodial activity in human and murine hepatocytes induced by gamma interferon and the parasite itself: enhancement by exogenous tetrahydrobiopterin. Infect. Immun. 62, 4043–4046.

Mitchell, H., Choudhury, A., Pagano, R.E., Leof, E.B., 2004. Ligand-dependent and -independent transforming growth factor-beta receptor recycling regulated by clathrin-mediated endocytosis and Rab11. Mol. Biol. Cell 15, 4166–4178.

Murray, J.D., 2002. Mathematical Biology. Springer, New York.

Nahrevanian, H., 2006. Immune effector mechanisms of the nitric oxide pathway in malaria: cytotoxicity versus cytoprotection. Braz. J. Infect. Dis. 10, 283–292.

Naotunne, T.S., Karunaweera, N.D., Mendis, K.N., Carter, R., 1993. Cytokine-mediated inactivation of malarial gametocytes is dependent on the presence of white blood cells and involves reactive nitrogen intermediates. Immunology 78, 555–562.

Novak, B., Tyson, J.J., 2008. Design principles of biochemical oscillators. Nat. Rev. Mol. Cell Biol. 9, 981–991.

Omer, F.M., de Souza, J.B., Riley, E.M., 2003. Differential induction of TGF-beta regulates proinflammatory cytokine production and determines the outcome of lethal and nonlethal Plasmodium yoelii infections. J. Immunol. 171, 5430–5436.

Omer, F.M., Kurtzhals, J.A., Riley, E.M., 2000. Maintaining the immunological balance in parasitic infections: a role for TGF-β? Parasitol. Today 16, 18–23.

Pakpour, N., Akman-Anderson, L., Vodovotz, Y., Luckhart, S., 2013. The effects of ingested mammalian blood factors on arthropod immunity and physiology. Microbes. Infect. 15, 243–254.

Patel, S.N., Lu, Z., Ayi, K., Serghides, L., Gowda, D.C., Kain, K.C., 2007. Disruption of CD36 impairs cytokine response to *Plasmodium falciparum* glycosylphosphatidylinositol and confers susceptibility to severe and fatal malaria *in vivo*. J Immunol. 178, 3954–3961.

Pearson, K., 1901. On lines and planes of closest fit to systems of points in space. Philos. Mag. 2, 559–572.

Peterson, T.M., Gow, A.J., Luckhart, S., 2007. Nitric oxide metabolites induced in *Anopheles stephensi* control malaria parasite infection. Free Radical Biol. Med. 42, 132–142.

Pinzar, E., Wang, T., Garrido, M.R., Xu, W., Levy, P., Bottari, S.P., 2005. Angiotensin II induces tyrosine nitration and activation of ERK1/2 in vascular smooth muscle cells. FEBS Lett. 579, 5100–5104.

Porras, M., Martin, M.T., Torres, R., Vergara, P., 2006. Cyclical upregulated iNOS and long-term downregulated nNOS are the bases for relapse and quiescent phases in a rat model of IBD. Am. J. Physiol. Gastrointest. Liver Physiol. 290, G423–G430.

Roberts, A.B., Sporn, M.B., 1990. The transforming growth factor-βs. In: Sporn, M.B., Roberts, A.B. (Eds.), Peptide Growth Factors and their Receptors. Springer-Verlag, Springer-Verlag, pp. 419–472, pp. 419–472.

Roberts, A.B., Sporn, M.B., 1996. Transforming growth factor-β. In: Clark, R.A.F. (Ed.), The Molecular and Cellular Biology of Wound Repair. Plenum Press, Plenum Press, pp. 275–308, pp. 275–308.

Surachetpong, W., Pakpour, N., Cheung, K.W., Luckhart, S., 2011. Reactive oxygen species-dependent cell signaling regulates the mosquito immune response to *Plasmodium falciparum*. Antioxid. Redox Signal. 14, 943–955.

Surachetpong, W., Singh, N., Cheung, K.W., Luckhart, S., 2009. MAPK ERK signaling regulates the TGF-beta1-dependent mosquito response to *Plasmodium falciparum*. PLoS Pathog. 5, e1000366.

Tarantola, A., 2005. Inverse problem theory and methods for model parameter estimation. Society for Industrial and Applied Mathematics, Philadelphia, PA.

Vilar, J.M., Saiz, L., 2011. Trafficking coordinate description of intracellular transport control of signaling networks. Biophys. J. 101, 2315–2323.

Vodovotz, Y., 1997. Control of nitric oxide production by transforming growth factor-β1: mechanistic insights and potential relevance to human disease. Nitric Oxide: Biol. and Chem. 1, 3–17.

Vodovotz, Y., Chesler, L., Chong, H., Kim, S.J., Simpson, J.T., DeGraff, W., Cox, G.W., Roberts, A.B., Wink, D.A., Barcellos-Hoff, M.H., 1999. Regulation of transforming growth factor-β1 by nitric oxide. Cancer Res. 59, 2142–2149.

Vodovotz, Y., Zamora, R., Lieber, M.J., Luckhart, S., 2004. Cross-talk between nitric oxide and transforming growth factor-β1 in malaria. Curr. Mol. Med. 4, 787–797.

Voordouw, M.J., Koella, J.C., Hurd, H., 2008. Comparison of male reproductive success in malaria-refractory and susceptible strains of *Anopheles gambiae*. Malar. J. 7, 103.

Wahl, S.M., 2007. Transforming growth factor-beta: innately bipolar. Curr. Opin. Immunol. 19, 55–62.

Weber, T.J., Shankaran, H., Wiley, H.S., Opresko, L.K., Chrisler, W.B., Quesenberry, R. D., 2010. Basic fibroblast growth factor regulates persistent ERK oscillations in premalignant but not malignant JB6 cells. J. Invest. Dermatol. 130, 1444–1456.

WHO. World Malaria Report, 2011. Geneva, Switzerland, World Health Organization.

Zamora, R., Vodovotz, Y., 2005. Transforming growth factor-β in critical illness. Crit. Care Med. 33, S478–S481.

Zhu, J., Krishnegowda, G., Gowda, D.C., 2005. Induction of proinflammatory responses in macrophages by the glycosylphosphatidylinositols of *Plasmodium falciparum*: the requirement of extracellular signal-regulated kinase, p38, c-Jun *N*-terminal kinase and NF-kappaB pathways for the expression of proinflammatory cytokines and nitric oxide. J. Biol. Chem. 280, 8617–8627.

Please cite this article as: Price, I., et al., *In vivo*, *in vitro*, and *in silico* studies suggest a conserved immune module that regulates malaria parasite transmission from mammals to mosquitoes. J. Theor. Biol. (2013), http://dx.doi.org/10.1016/j.jtbi.2013.05.028